



# HHS Public Access

Author manuscript

*Int J Mass Spectrom.* Author manuscript; available in PMC 2016 November 15.

Published in final edited form as:

*Int J Mass Spectrom.* 2015 November 15; 390: 101–109. doi:10.1016/j.ijms.2015.07.013.

## In-Source Decay Characterization of Isoaspartate and $\beta$ -Peptides

Xiang Yu<sup>1,†</sup>, Nadezda P. Sargaeva<sup>1,†</sup>, Christopher J. Thompson<sup>2</sup>, Catherine E. Costello<sup>1</sup>, and Cheng Lin<sup>1,\*</sup>

<sup>1</sup>Mass Spectrometry Resource, Department of Biochemistry, Boston University School of Medicine, 670 Albany Street, Suite 504, Boston, MA 02118

<sup>2</sup>Bruker Daltonics, Inc., 40 Manning Road, Billerica, MA 01821

### Abstract

Deamidation and the subsequent formation of isoaspartic acid (isoAsp) are common modifications of asparagine (Asn) residues in proteins. Differentiation of isoAsp and Asp residues is a challenging task owing to their similar chemical properties and identical molecular mass. Recent studies showed that they can be differentiated using electron capture dissociation (ECD) which generates diagnostic fragments  $c'+57$  and  $z^*-57$  specific to the isoAsp residue. However, the ECD approach is only applicable towards multiply charged precursor ions and generally does not work for  $\beta$ -amino acids other than isoAsp. In this study, the potential of in-source decay (ISD) in characterization of isoAsp and other  $\beta$ -amino acids was explored. For isoAsp-containing peptides, ISD with a conventional hydrogen-donating matrix produced ECD-like,  $c'+57$  and  $z^*-57$  diagnostic ions, even for singly charged precursor ions. For other  $\beta$ -amino acids, a hydrogen-accepting matrix was used to induce formation of site-specific  $a-14$  ions from a synthetic  $\beta$ -analogue of substance P. These results indicated that ISD can be broadly applied for  $\beta$ -peptide characterization.

### Keywords

Isoaspartate;  $\beta$ -peptide; MALDI-ISD; TOF-MS; FTICR-MS

### Introduction

Isoaspartic acid (isoAsp) is an isomer of aspartic acid (Asp) that can be formed spontaneously under physiological conditions via isomerization of Asp or deamidation of asparagine (Asn) residues.<sup>1</sup> IsoAsp is a  $\beta$ -linked amino acid with an extra methylene group inserted into the peptide backbone. Such backbone elongation may alter the protein conformation leading to protein activity change, misfolding and degradation.<sup>2–4</sup> *In vivo*,

\*To whom correspondence should be addressed. Prof. Cheng Lin, Phone: +1 (617) 638 6705, Fax: +1 (617) 638 6761, chenglin@bu.edu.

<sup>†</sup>indicates equal contribution.

**Publisher's Disclaimer:** This is a PDF file of an unedited manuscript that has been accepted for publication. As a service to our customers we are providing this early version of the manuscript. The manuscript will undergo copyediting, typesetting, and review of the resulting proof before it is published in its final citable form. Please note that during the production process errors may be discovered which could affect the content, and all legal disclaimers that apply to the journal pertain.

isoAsp accumulation in long-lived proteins is often associated with aging,<sup>2</sup> eye lens abnormalities,<sup>5</sup> and amyloid diseases such as Alzheimer disease.<sup>3,6</sup> *In vitro*, isoAsp formation is a major concern in the biopharmaceutical industry, potentially leading to protein aggregation and activity loss.<sup>7</sup>

Many analytical tools have been developed for isoAsp characterization in peptides and proteins.<sup>6,8-17</sup> Among them, the best results were achieved using the high performance liquid chromatography (HPLC)<sup>13,18-21</sup> and tandem mass spectrometry (MS) methods.<sup>22-31</sup> Recently, electron activated dissociation (ExD) methods, including electron capture dissociation (ECD) and electron transfer dissociation (ETD), have been successfully applied to isoAsp analysis,<sup>14,32-33</sup> where site-specific isoAsp detection was achieved based on the formation of the diagnostic  $c'+57$  and  $z^*-57$  ions resulting from the  $C_{\alpha}$ - $C_{\beta}$  bond cleavage within the isoAsp residue. Both ECD and ETD involve charge reduction, and are therefore limited to analysis of multiply charged precursor ions, typically generated by electrospray ionization (ESI). They are not applicable towards singly charged ions that dominate matrix-assisted laser desorption/ionization (MALDI) mass spectra.

The presence of a  $C_{\alpha}$ - $C_{\beta}$  bond on the peptide backbone is a structural feature of all  $\beta$ -amino acids. Like isoAsp, a  $\beta$ -amino acid has an extra methylene group incorporated between its amino and carboxylate groups. There are two types of  $\beta$ -amino acids:  $\beta_2$  and  $\beta_3$ , with the side chain attached to the  $\alpha$ - and  $\beta$ -carbon respectively.  $\beta$ -amino acids do not normally occur in nature except for  $\beta$ -aspartate (isoAsp) and  $\beta$ -alanine, the latter being a component of pantothenic acid, of coenzyme A, and of carnosine in muscle tissue. Neither do  $\beta$ -peptides exist in nature, but they can be synthesized.<sup>34-35</sup> A biologically important property of  $\beta$ -peptides is their stability against proteolytic degradation in human and other living organisms.<sup>36-38</sup> Synthetic  $\beta$ -peptides designed to resemble the epitopes of natural peptides to mimic their functions can be used as agonists and antagonists in peptide-protein, protein-protein, and peptide-DNA/RNA interactions.<sup>39-41</sup> These features provide  $\beta$ -peptides with great potential as proteolytically stable therapeutics and antibiotics for antibiotic-resistant pathogens.

Circular dichroism spectroscopy, X-ray crystallography and nuclear magnetic resonance spectroscopy are the primary tools used to study the structure of  $\beta$ -peptides.<sup>34,37,39,42</sup> Radioactive labeling, HPLC and MALDI mass spectrometry have also been applied to monitor  $\beta$ -peptides in tissues.<sup>36,38</sup> However, a fast and accurate analytical method capable of distinguishing  $\alpha$ - from  $\beta$ -, and  $\beta_2$ - from  $\beta_3$ - type amino acids is still lacking. As ExD has shown great utility for isoAsp analysis, it would seem to be an ideal tool for characterizing other  $\beta$ -amino acids as well. To date, however, attempts to apply ExD in  $\beta$ -peptide analyses have largely failed.<sup>43-44</sup> With the exception of  $\beta$ -phenylalanine ( $\beta$ -Phe) and isoAsp, ExD produced neither  $N$ - $C_{\beta}$  nor  $C_{\alpha}$ - $C_{\beta}$  cleavage at  $\beta$ -linkage sites. It appears that formation of isoAsp diagnostic ions is driven by the stability of the radical  $c'+57$  ion due to the presence of the side-chain carboxylic group. Such radical stabilization is absent in other  $\beta$ -amino acids, except for  $\beta$ -Phe. Therefore, there is still a need to develop alternative analytical methods to address this challenge.

MALDI in-source decay (ISD) is a pseudo tandem MS technique, which occurs as a result of the metastable decay of precursor ions during delayed extraction within the ion source.<sup>45–47</sup> ISD with common hydrogen-donating matrices generates predominantly  $c'$ - and  $z'$ -type ions, similar to those produced in ECD and ETD.<sup>48–49</sup> In addition, labile post-translational modifications (PTMs) are usually preserved in the ISD process. The ability to produce ECD-like fragments without charge reduction makes ISD an attractive alternative fragmentation method for MALDI-generated ions. ISD has been applied to analyze peptides and proteins with phosphorylation and *O*- and *N*-glycosylation, to differentiate the isomeric amino acid residues leucine and isoleucine, and to obtain information on disulfide-linkages.<sup>50–55</sup> Despite early speculation that ISD may result from electron capture by the multiply-charged molecular species in the MALDI plume,<sup>56</sup> it is now generally accepted that ISD is initiated by hydrogen transfer from the matrix molecule to the backbone carbonyl oxygen.<sup>48</sup> A number of matrices have been tested for ISD experiments, including picolinic acid (PA), 1,5-diaminonaphthalene (1,5-DAN), and 2,5-dihydroxybenzoic acid (DHB).<sup>57</sup> It was found that the ISD efficiency is generally enhanced by increasing the hydrogen-donating ability of the matrix molecule.<sup>57</sup> Recently, Takayama and coworkers reported that the use of hydrogen-accepting matrices, such as 5-formylsalicylic acid (5-FSA), 5-nitrosalicylic acid (5-NSA) and 2,5-bis(2-hydroxyethoxy)-7,7,8,8-tetracyanoquinodimethane (bisHE-TCNQ), may also lead to efficient ISD, initiated by the abstraction of a hydrogen atom from the backbone amide nitrogen, producing primarily  $a$ - and  $x$ -type ions.<sup>58–61</sup>

In this work, the potential of ISD for characterization of isoAsp and other  $\beta$ -amino acid residues was investigated using MALDI-Fourier transform ion cyclotron resonance (FTICR) MS and MALDI-time-of-flight (TOF) MS.

## Experimental

### Peptides and Reagents

Substance P,  $\beta$ -2-microglobulin from human urine ( $\beta$ 2M), endoproteinase Glu-C (Glu-C), and MALDI matrices, including 5-NSA, 1,5-DAN, and 2-PA were purchased from Sigma-Aldrich (St. Louis, MO). C-terminally amidated substance P with two amino acids modified to  $\beta_3$ -homo amino acids (RPKP $\beta$ hQQFFG $\beta$ hLM-NH<sub>2</sub>, structure shown in Supporting Scheme S1) was custom synthesized by AnaSpec (San Jose, CA, USA). A  $\beta$ -homo amino acid has an extra methylene group along its backbone, while its side chain group stays the same. Formic acid (FA) and trifluoroacetic acid (TFA) were obtained from Thermo Scientific (Rockford, IL). HPLC grade acetonitrile (ACN) and methanol (MeOH) were obtained from Fisher Scientific (Fair Lawn, NJ, USA).

### Reductive Alkylation, Protein Aging and Proteolysis

$\beta$ 2M was reduced, alkylated, and desalted using Poros 50 R1 material (Thermo Scientific, CA) as described previously.<sup>62</sup> It was then incubated in the ammonium bicarbonate buffer solution (pH 7.8) at 37 °C for 7 days. The aged  $\beta$ 2M was desalted again followed by digestion with Glu-C at 1:50 (w:w) enzyme/protein ratio in the ammonium acetate buffer solution (pH 4.0) at 37 °C for 16 hr.

## Reversed Phase High Performance Liquid Chromatography (RP-HPLC)

The Glu-C digest of the aged  $\beta$ 2M was separated on a Vydac 218TP5215 reversed phase C18 column ( $4.6 \times 250$  mm) using an Agilent 1200 Series HPLC system (Agilent Technologies, Wilmington, DE). Mobile phase A was 99% water, 1% ACN, and 0.1% TFA, and mobile phase B was 99% ACN, 1% water, and 0.1% TFA. A linear gradient of 5% to 95% of mobile phase B in 30 min was used at a flow rate of 1 mL/min at 30 °C. The chromatograms were obtained with UV detection at 214 nm and fractions were collected at 4 °C and dried before MS analysis.

## MALDI Sample Preparation

Peptides were dissolved in 50:50 ACN:H<sub>2</sub>O (v:v) with 0.1 % FA to a concentration of 20–100 pmol/ $\mu$ L. The 5-NSA, 1,5-DAN, and 2-PA matrices were prepared freshly in 50:50 ACN:H<sub>2</sub>O (v:v) with 0.1 % FA at a concentration of 20 mg/mL. The 1,5-DAN and 2-PA solutions were then mixed at a ratio of 3:1 (v:v) as recommended by a previous report.<sup>57</sup> The “sandwich” method was used for sample deposition onto a stainless steel target plate by adding 0.5  $\mu$ L of matrix solution, 1  $\mu$ L of analyte solution, and 0.5  $\mu$ L of matrix solution sequentially, letting the droplet dry each time before spotting the following layer.

## Mass Spectrometry

The ISD experiments were performed on either an ultrafleXtreme™ MALDI-TOF/TOF instrument (Bruker Daltonics, Bremen, Germany), or an ESI/MALDI dual-source solariX™ hybrid Qh-FTICR instrument (Bruker Daltonics, Bremen, Germany) with a 12-T actively shielded magnet. Both instruments are equipped with a smartbeam™-II laser (355 nm, 3-nsec pulse width, power level 100  $\mu$ J/pulse, repetition rate 1 kHz). A typical ISD-TOF mass spectrum was obtained by summing 20 acquisitions, at 500 laser shots per acquisition, with the laser power set at 30% to 45%. The ISD-FTICR mass spectra were acquired with 25–30% laser power, at 500–1000 laser shots per scan. A 0.8-s transient was typically acquired for each scan and up to 16 scans were accumulated for each spectrum to improve the S/N ratio. All spectra were zero-filled once, Fourier transformed with sine-bell apodization, and processed using the DataAnalysis 4.0 software. The MS/MS spectra were calibrated internally with fragment ions that were assigned with high confidence.

## Nomenclature

To keep track of the hydrogen atom transfer to and from the ISD fragments, we adopted here the Zubarev notation.<sup>63</sup> In this notation, fragment ions resulted from the homolytic cleavage of a chemical bond are denoted by the radical sign ‘•’, *e.g.* homolytic N-C $\alpha$  bond cleavage generates *c*• and *z*• ions, and homolytic C $\alpha$ -C(=O) cleavage produces *a*• and *x*• ions. The radical sign is removed following the loss of a hydrogen atom from the fragment, or replaced by the prime sign ‘’ when a hydrogen atom is transferred to the radical fragment.

## Results and Discussion

### Isoaspartate Characterization by ISD

For bottom-up isoAsp analysis, the endoproteinase Glu-C was used because it generated longer isoAsp-containing peptides from  $\beta$ 2M than trypsin. This is advantageous for MALDI-ISD studies as the low-mass region of a MALDI spectrum is often dominated by matrix cluster peaks that can interfere with sequence ion detection. Figures 1 and 2 show the ISD spectra of two Glu-C peptides,  $\beta$ 2M 1–36 and  $\beta$ 2M 78–99, from the reduced, alkylated and aged  $\beta$ 2M, acquired with the 1,5-DAN/2-PA matrix on the FTICR-MS instrument.  $\beta$ 2M 1–36 and  $\beta$ 2M 78–99 were the only major component in their respective HPLC fraction spotted on the MALDI target (Supporting Figure S1). HPLC separation prior to ISD analysis was necessary because precursor ion selection cannot be achieved in ISD. For  $\beta$ 2M 1–36, a continuous series of  $c'$ -ions from  $c_{5'}$  to  $c_{33'}$  were observed, except for those requiring N- $C_{\alpha}$  bond cleavage on the N-terminal side of a proline residue (Figure 1). For  $\beta$ 2M 78–99, ISD cleaved 18 out of 21 inter-residue N- $C_{\alpha}$  bonds, with most cleavages producing complementary  $c'$ - and  $z'$ -ions (Figure 2).

The resemblance of the ISD fragmentation pattern to that of ECD suggests that ISD likely follows a fragmentation pathway similar to ECD. It was proposed that ISD is initiated by the intermolecular hydrogen transfer from the matrix molecule to the precursor ion, producing a carbon-centered radical intermediate that subsequently undergoes alpha cleavage on its C-terminal side and generates  $c'$ - and  $z^*$ -type ions (Scheme 1a). If this ISD mechanism holds true, for isoAsp-containing peptides, the carbon radical could also induce alpha cleavage on its N-terminal side, leading to  $C_{\alpha}$ - $C_{\beta}$  bond cleavage within the isoAsp residue and production of the diagnostic  $c'+57$  and  $z^*-57$  ions (Scheme 1b). Indeed, the isoAsp17 diagnostic ion,  $c_{16}'+57$ , was observed in the ISD spectrum of the aged  $\beta$ 2M peptide 1–36, but not in that of the unaged sample (Figure 1, insets a, b). Similarly, the isoAsp83 diagnostic ion,  $z_{17}^*-57$ , was observed in the ISD spectrum of the aged  $\beta$ 2M peptide 78–99 (Figure 2, inset). These results established ISD as a viable method for isoAsp detection. However, because it requires off-line HPLC separation, the ISD approach is not a high-throughput method, and may compare unfavorably to the on-line LC-ECD/ETD-MS/MS approach for isoAsp analysis, particularly on the omics scale. Nonetheless, in applications where the sample is not too complex and high throughput is not required, *e.g.* in the study of Asn deamidation in a specific therapeutic protein, it is practical to carry out off-line HPLC separation before ISD analysis of the fraction(s) of interest. One advantage of ISD is that, as an off-line method, it allows extensive signal averaging. This can be especially beneficial for isoAsp analysis, as the diagnostic ions are often produced in low abundance, and may not be detectable during on-line LC-MS/MS analysis.

As previously reported, enzymatic digestion can sometimes lead to *in vitro* Asn deamidation and isoAsp formation during sample preparation.<sup>17</sup> These undesirable artifacts may be minimized by using the top-down approach where the protein is analyzed directly without proteolysis. It has been shown that ECD can generate isoAsp diagnostic ions at the intact protein level, but this was challenging because the product ion signals were distributed over many competing fragmentation channels and the extensive non-covalent interaction within a

protein molecule could hinder diagnostic ion formation and detection.<sup>62</sup> Similarly observed here, isoAsp diagnostic ions were not initially detected in the MALDI-ISD spectrum of the aged  $\beta$ 2M protein. However, because ISD takes place in the ionization source region before the mass filtering quadrupole, it is possible to selectively isolate and externally accumulate ions within a small  $m/z$  window before transferring them into the ICR cell for mass analysis. Such continuous accumulation of selected ions (CASI<sup>TM</sup>) in an external ion storage device allows detection of low-abundance ions that are otherwise difficult to observe due to the limited storage capacity of the collision cell. Figure 3 shows a single-scan MALDI-ISD spectrum of aged  $\beta$ 2M protein with external accumulation of fragment ions in the  $m/z$  range of 1850 to 2050 over 100 laser shots. The isoAsp17 diagnostic ion,  $c_{16}'+57$ , was easily detected with high mass accuracy and a signal-to-noise ratio of 55. With minimum sample preparation and rapid spectral acquisition, top-down MALDI-ISD analysis with CASI can potentially serve as a screening method for isoAsp detection using a targeted approach.

### ISD of Other $\beta$ -Amino Acid Residues with Hydrogen-Donating Matrices

For  $\beta$ -amino acids other than isoAsp and  $\beta$ -Phe, ECD failed to produce the diagnostic  $C_{\alpha}$ - $C_{\beta}$  or the N- $C_{\beta}$  bond cleavage because the resulting  $\beta$ -carbon radical could no longer be stabilized by the side chain group.<sup>43-44</sup> Since ISD with hydrogen-donating matrices proceeds via the same carbon-centered radical, a similar lack of N- $C_{\beta}$  and  $C_{\alpha}$ - $C_{\beta}$  cleavages was expected in ISD of  $\beta$ -peptides. Surprisingly, with the 1,5-DAN/2-PA matrix, ISD of the  $\beta$ -substance P analogue generated both  $c_4'$  and  $c_9'$  ions resulting from the N- $C_{\beta}$  bond cleavage at the two  $\beta$ -linkage sites (Figure 4, insets a and b). More importantly, ISD was able to cleave  $C_{\alpha}$ - $C_{\beta}$  bonds at the two  $\beta$ -linkage sites, producing  $c_4'+83$  and  $c_9'+68$  ions, respectively (Figure 4, insets c and d). However, unlike the radical  $c'+57$  ions observed in the ECD and ISD spectra of isoAsp-containing peptides, the  $c_4'+83$  and  $c_9'+68$  ions are even-electron species, suggesting that their formation likely followed a different pathway. Note that N-terminal fragments resulting from  $C_{\alpha}$ - $C_{\beta}$  cleavage within a  $\beta_3$ -amino acid residue can be generally described as  $a$ -CH<sub>2</sub> or  $a$ -14 ions. It appears that  $a$ -14 ions were specific to  $\beta_3$ -linkages, as they were absent in all other sites, *e.g.* Figure 4, inset e.

Aside from the  $c'$ -ion series, ISD of  $\beta$ -substance P also produced an extensive series of  $a$ -ions. Enhanced  $a^*/y$  ion formation is a feature in ECD of  $\beta$ -peptides, which is believed to be initiated by electron capture at the backbone amide nitrogen protonation sites, when the primary  $c'/z^*$  fragmentation pathway is suppressed.<sup>44</sup> Here, however, abundant  $a$ -ion formation was not limited to  $\beta$ -linkage sites. Moreover, unlike ECD which generated primarily odd-electron  $a^*$ -ions, ISD produced exclusively even-electron  $a$ -ions. It was proposed that, in ISD, an  $a^*$ -ion is formed via an oxygen-centered radical intermediate (Supporting Scheme S2).<sup>64-65</sup> An  $a^*$ -ion then loses a hydrogen atom to produce the even-electron  $a$ -ion, presumably via hydrogen abstraction by the radical species present in the MALDI plume. Finally, secondary side chain loss from some  $a^*$ -ions was also observed (Figure 4, insets f and g), providing additional evidence for the involvement of odd-electron  $a^*$  intermediates in ISD. Note that side chain losses from  $a^*$ -ions are useful for differentiation of  $\beta_2$ - and  $\beta_3$ -linked amino acid residues (Supporting Scheme S3).



## ISD of $\beta$ -Linked Peptides with Hydrogen-Accepting Matrices

If fragments derived from  $a^{\bullet}$ -ions are useful for  $\beta$ -amino acid characterization, it may be advantageous to perform ISD with hydrogen-accepting matrices. During the MALDI process, the hydrogen-accepting matrix molecule can abstract a hydrogen atom from the backbone nitrogen, generating a hydrogen-deficient amide nitrogen radical intermediate. For  $\alpha$ -linked amino acid residues, the subsequent radical-induced cleavage to the N-terminal side of the nitrogen radical breaks the  $C_{\alpha}$ -C(=O) bond, producing  $a^{\bullet}$ - and  $x$ -ions (Scheme 2a). Further hydrogen abstraction from an  $a^{\bullet}$ -ions forms an even-electron  $a$ -ion.

Alternatively, the nitrogen radical can induce  $\alpha$ -cleavage on its C-terminal side, leading to the formation of  $a$ - and  $x^{\bullet}$ -ions (Scheme 2b), although the  $a/x^{\bullet}$  fragmentation pathway is both energetically and kinetically unfavored.<sup>59,66–67</sup> For  $\beta_3$ -linked amino acid residues, however,  $\alpha$ -cleavage on the C-terminal side of the nitrogen radical would lead to the breakage of the  $C_{\alpha}$ - $C_{\beta}$  bond, generating  $a-14$  and  $x^{\bullet}+14$  ions (Scheme 2c). The radical stays on the alpha carbon of the C-terminal fragment, which should be stabilized by the backbone carbonyl, regardless of the side chain of the amino acid residue involved. To test this hypothesis, the synthetic  $\beta$ -substance P analogue was subjected to ISD-FTICR analysis using the 5-NSA matrix. The resulting ISD spectrum (Figure 5) was dominated by  $a$ -type ions. Several  $a$ -ions were also accompanied by additional side-chain losses, e.g.  $a_6^{\bullet}$ - $C_2H_4NO$ , and  $a_{10}^{\bullet}$ - $C_4H_9$ . These side-chain losses were not specific to  $\beta$ -amino acid residues, and likely resulted from secondary radical-induced fragmentation of  $a^{\bullet}$ -ions. Some low-abundance  $c'$ -ions were also produced, possibly owing to the presence of a hydroxyl and a carboxyl groups in 5-NSA that can serve as hydrogen donors. In addition, all sequence ions were accompanied by their doubly hydrogen loss forms, and this is characteristic of ISD with hydrogen-accepting matrices.<sup>58</sup> Finally, as predicted, ISD with 5-NSA generated two  $\beta$ -amino acid specific fragments,  $a_5-14$  and  $a_{10}-14$ , resulting from the  $C_{\alpha}$ - $C_{\beta}$  bond cleavage within the  $\beta$ h-Gln5 and  $\beta$ h-Leu10 residues, respectively (Figure 5, insets a, b). No  $CH_2$  loss was observed in other  $a$ -ions (e.g. Figure 5, inset c) or in any  $a$ -ions from ISD of  $\alpha$ -substance P (Figure S2, insets), indicating that  $a-14$  ions are diagnostic for  $\beta_3$ -linked amino acid residues in ISD spectra with hydrogen-accepting matrices.

## Comparison of ISD Performances on FTICR MS and TOF MS Instruments

The ISD spectra presented thus far were all acquired on an FTICR mass spectrometer. A MALDI-FTICR instrument offers two advantages over a MALDI-TOF instrument for ISD analysis. First, matrix cluster ions are commonly observed in MALDI-TOF mass spectra, and often dominate the low-mass region, preventing reliable identification of ions with low  $m/z$  values, particularly when analyte ions are present at low abundance. Meanwhile, it is usually possible to separate the peak of interest from matrix interference peaks using an ICR mass analyzer owing to its superior mass resolving power and mass accuracy. Figures 4 and S3 show the ISD spectra of the  $\beta$ -substance P peptide, obtained on the FTICR and on the TOF instrument, respectively. In the MALDI-TOF spectrum, some sequence ions have significant overlaps with matrix peaks, and cannot be positively identified (e.g.  $c_5'$ , Figure S3, inset). Although the MALDI-FTICR spectrum also contains many matrix cluster peaks in the low-mass region, one can easily differentiate the sequence ions from matrix cluster ions based on the accurate mass measurement (Figure 4, insets a, h). Second, ISD spectra are

typically acquired with high laser power, resulting in a wider spread of ion kinetic energy. This presents a particularly severe problem for axial-TOF instruments, as it leads to poor mass resolving power and low mass accuracy. The MALDI-o-TOF instrument shows significantly improved ISD performance over the axial TOF instrument, because the ions are cooled and focused by buffer gas, and injected orthogonally into the flight tube, minimizing the deleterious effect of the axial kinetic energy spread.<sup>68</sup> Similarly, because an ICR mass analyzer determines the  $m/z$  value of an ion based on its cyclotron frequency, which is independent of its axial velocity, the mass resolving power is not compromised by the broader kinetic energy spread.

Despite its superior performance, the MALDI-FTICR MS instrument is not widely available. It is thus important to study the ISD fragmentation behavior of  $\beta$ -peptides on the more accessible MALDI-TOF mass spectrometers. Figure 6 shows the zoomed-in view of several regions of interest in the ISD spectra of  $\beta$ -substance P obtained with the 1,5-DAN/2-PA and 5-NSA matrices, and on the TOF and FTICR instruments, respectively. The percentage number in each spectral view corresponds to the relative abundance of that ion to the most abundant primary sequence ion observed, which was  $c_6'$  in the ISD-TOF spectrum with the 1,5-DAN/2-PA matrix, and  $a_8$  in all other spectra. For experiments performed on the TOF instrument, the ISD fragmentation behavior of this peptide differed significantly depending on the matrix used, and was generally consistent with the mechanisms proposed in Schemes 1 and 2. As formation of  $c'$ -ions, *e.g.*  $c_7'$ , was initiated by the hydrogen transfer to the backbone carbonyl, they were more abundantly present in the ISD spectra obtained with the 1,5-DAN/2-PA matrix due to its greater hydrogen-donating ability. On the other hand,  $a$ -ions (*e.g.*  $a_6$ ) and their side chain loss products (*e.g.*  $a_{10}^{\bullet}$ -C<sub>4</sub>H<sub>9</sub>), as well as the  $\beta_3$ -linkage specific  $a$ -14 ions (*e.g.*  $a_{10-14}$ ), were much more abundantly produced by ISD with the 5-NSA matrix, as their formation likely required hydrogen abstraction from the backbone amide nitrogen (Schemes 2 and S3). The ISD-FTICR mass spectra acquired with these two matrices, however, were much more similar. In particular, the 1,5-DAN/2-PA spectrum contained many  $a$ -type fragment ions that were typically formed in ISD with a hydrogen-accepting matrix.

To rationalize the difference between the ISD spectra acquired on the MALDI-TOF and the MALDI-FTICR instruments, it is important to note that these two instruments not only employ different mass analyzers, but also have different ion source pressures. Whereas the TOF instrument has a vacuum MALDI source, the MALDI source in the FTICR instrument was operated at an intermediate pressure of around 2.5 mbar. The elevated pressure in the ion source region would lead to frequent collisions between the analyte and background gas, resulting in both collisional cooling and collisional activation depending on the collision energy and pressure.<sup>51,54,68</sup> For ISD with hydrogen-donating matrices, Asakawa and coworkers showed that the hydrogen transfer from the matrix molecule to the carbonyl oxygen of the peptide backbone occurred primarily on the matrix crystal before desorption, leading to the formation of  $c'$ - and  $z^*$ -type ions upon N-C <sub>$\alpha$</sub>  bond cleavage.<sup>65</sup> Consequently, the abundance of  $c'$ -ions should not be significantly affected by the source pressure, as observed here (Figure 6). A notable exception is  $c_9'$  whose abundance was greatly enhanced in the FTICR spectra. Formation of  $c_9'$  upon N-C <sub>$\beta$</sub>  bond cleavage following hydrogen



transfer to the backbone carbonyl oxygen is an unfavored process as it is accompanied by the production of  $z_2^\bullet$  whose radical site is on the  $\beta$ -carbon and not resonantly stabilized. Thus, only a very low abundance  $c_9'$  peak was observed in the ISD-TOF spectra of  $\beta$ -substance P. An increase in the propensity to form the  $c'$ -ion at higher source pressure was previously reported by Dreisewerd and coworkers, who attributed the increased yield of  $c'$ -ions to the stabilization of the internally excited fragment ions by collisional cooling.<sup>68</sup> Thermal stabilization of labile biomolecules had earlier been reported by O'Connor and Costello using elevated pressure in an MALDI-FTICR instrument.<sup>69</sup> However, it is unclear why the collisional cooling effect was much more pronounced for  $c_9'$  if it was formed via the mechanism shown in Scheme 1a, since  $c_9'$  is a stable even-electron species like other  $c'$ -ions formed upon N-C $_{\alpha}$  bond cleavages. We propose here an alternative pathway, where  $c_9'$  was formed from  $a_{10}^\bullet$  upon N-C $_{\beta}$  bond cleavage and hydrogen transfer (Scheme S4a). As formation of  $a^\bullet$ -ions in ISD with a hydrogen-donating matrix proceeds via an oxygen-centered radical and requires substantial ion activation, it is reasonable to expect high-abundance  $c_9'$  ion only when ISD is performed at higher pressure in a MALDI source where collisional activation takes place. Frequent collisions may also have facilitated hydrogen transfer to the  $c_9^\bullet$ -ion to form the  $c_9'$ -ion. Similarly, formation of other  $a^\bullet$ -derived fragment ions, such as  $a_{10}^\bullet$ -C $_4$ H $_9$  (Scheme S4b), was also greatly enhanced in the ISD-FTICR spectrum with the 1,5-DAN/2-PA matrix. With a hydrogen-accepting matrix, however,  $a^\bullet$ -ions were formed via amide nitrogen radical intermediates (Scheme 2a), which required no ion activation. Consequently, when using 5-NSA as the matrix,  $a^\bullet$ -ions and  $a^\bullet$ -derived ions were abundantly present in the ISD spectra acquired on both instruments. Formation of the  $\beta_3$ -linkage specific  $a$ -14 ions is a special case, as they were not derived from  $a^\bullet$  ions. Their appearance in the ISD spectra with the 5-NSA matrix has been rationalized in Scheme 2c. Interestingly, when performed in the elevated pressure MALDI source, ISD with the 1,5-DAN/2-PA matrix also produced abundant  $a$ -14 ions. Although neither 1,5-DAN nor 2-PA was an effective hydrogen acceptor, the MALDI plume likely contained many radical species that could abstract a hydrogen from the peptide backbone amide nitrogen, particularly when the ion source is operated at higher pressures where collisions abounded, producing an ISD spectrum similar to the one obtained with a hydrogen-accepting matrix.

Finally, it is worth noting that there is also a vast difference in timeframes between these two instruments. The longer delay between ion generation and ion detection in the FTICR instrument (typically in hundreds of milliseconds) than that in the TOF instrument (typically in tens of microseconds) may also account for some of the differences observed between the ISD spectra obtained on these instruments. For example, the matrix cluster ions were present at lower abundances in the FTICR spectra than in the TOF spectra (*e.g.* Figures 4 and S3), possibly because of their decomposition before detection. Furthermore, it is possible that some secondary fragment ions were generated after the primary ISD fragments exited the source region (*e.g.*  $a_{10}^\bullet$  to  $a_{10}^\bullet$ -C $_4$ H $_9$ , Scheme S4b). If this was the case, the secondary ions would not be detected by the TOF/TOF analyzer, as they were essentially PSD fragments and would have required different reflectron focusing conditions to be detected. However, the difference in timeframes is unlikely the major contributing factor to the different ISD fragmentation patterns produced by these two instruments, as most ISD ions observed here should be generated by rapid radical-induced fragmentation processes. In addition, some

fragment ions that exhibited large difference in ion abundances between spectra obtained on these two instruments had to be produced in the ion source. For example, formation of  $c_9'$  from  $a_{10}^*$  required hydrogen transfer to the ISD fragment (Scheme S4a). Future experiments performed on a vacuum-MALDI-FTICR instrument may help to differentiate the effect of pressure and timeframe on the ISD fragmentation pattern.

## Conclusions

In this study, the potential of ISD in characterization of  $\beta$ -amino acids was investigated. Our results demonstrated that, ISD with a hydrogen-donating matrix can cleave the  $C_\alpha$ - $C_\beta$  bond and produce  $c'+57$  and  $z^*-57$  diagnostic ions for isoAsp identification. ISD with a hydrogen-accepting matrix, on the other hand, can produce a hydrogen-deficient backbone amide nitrogen radical, leading to  $C_\alpha$ - $C_\beta$  bond cleavage and formation of the  $a-14$  diagnostic ion at  $\beta_3$ -linkage sites. The resulting radical is stabilized by the backbone carbonyl group regardless of the side chain group, thus ISD with a hydrogen-accepting matrix can be used as a general method for  $\beta$ -amino acid characterization. MALDI-FTICR MS is better suited for  $\beta$ -peptide characterization, because its high mass resolving power and mass accuracy allow for more confident diagnostic ion assignment. Finally, if the MALDI ion source is operated at an elevated pressure, ISD with a conventional hydrogen-donating matrix can produce fragments that are normally only generated using a hydrogen-accepting matrix.

## Supplementary Material

Refer to Web version on PubMed Central for supplementary material.

## Acknowledgments

This work is supported by the NIH grants P41 RR10888/GM104603, R01 GM078293, S10 RR025082, and S10 OD010724.

## References

1. Robinson, NE.; Robinson, AB. Molecular clocks: Deamidation of asparaginy and glutaminy residues in peptides and proteins. Cave Junction, OR: Althouse Press; 2004. p. 443
2. Ritz-Timme S, Collins MJ. Racemization of aspartic acid in human proteins. Ageing Research Reviews. 2002; 1:43–59. [PubMed: 12039448]
3. Roher AE, Lowenson JD, Clarke S, Wolkow C, Wang R, Cotter RJ, Reardon IM, Zurcherneely HA, Heinrichson RL, Ball MJ, Greenberg BD. Structural alterations in the peptide backbone of beta-amyloid core protein may account for its deposition and stability in Alzheimer's disease. J. Biol. Chem. 1993; 268:3072–3083. [PubMed: 8428986]
4. Shimizu T, Watanabe A, Ogawara M, Mori H, Shirasawa T. Isoaspartate formation and neurodegeneration in Alzheimer's disease. Arch. Biochem. Biophys. 2000; 381:225–234. [PubMed: 11032409]
5. Fujii N, Ishibashi Y, Satoh K, Fujino M, Harada K. Simultaneous racemization and isomerization at specific aspartic acid residues in alpha B-crystallin from the aged human lens. Biochim. Biophys. Acta. 1994; 1204:157–163. [PubMed: 8142454]
6. Shimizu T, Matsuoka Y, Shirasawa T. Biological significance of isoaspartate and its repair system. Biol. Pharm. Bull. 2005; 28:1590–1596. [PubMed: 16141521]
7. Wakankar AA, Borchardt RT. Formulation considerations for proteins susceptible to asparagine deamidation and aspartate isomerization. J. Pharm. Sci. 2006; 95:2321–2336. [PubMed: 16960822]

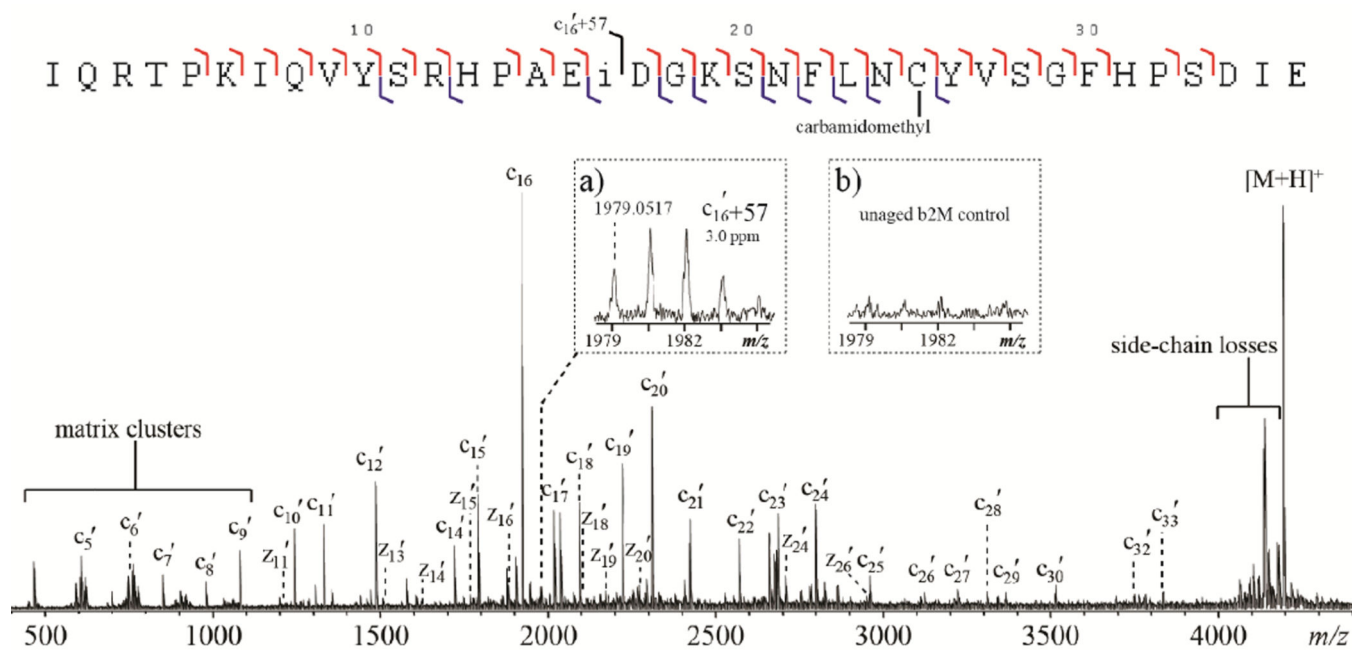
8. Di Donato A, Ciardiello MA, de Nigris M, Piccoli R, Mazzarella L, D'Alessio G. Selective deamidation of ribonuclease A. Isolation and characterization of the resulting isoaspartyl and aspartyl derivatives. *J. Biol. Chem.* 1993; 268:4745–4751. [PubMed: 8444851]
9. Aswad, DW.; Paranandi, MV.; Schurter, BT. 3rd Symposium on the Analysis of Well Characterized Biotechnology Pharmaceuticals. Washington, D.C.: Pergamon-Elsevier Science Ltd; 1999. p. 1129-1136.
10. Alfaro JF, Gillies LA, Sun HG, Dai SJ, Zang TZ, Klaene JJ, Kim BJ, Lowenson JD, Clarke SG, Karger BL, Zhou ZS. Chemo-enzymatic detection of protein isoaspartate using protein Isoaspartate methyltransferase and hydrazine trapping. *Anal. Chem.* 2008; 80:3882–3889. [PubMed: 18419136]
11. Shin Y, Cho HS, Fukumoto H, Shimizu T, Shirasawa T, Greenberg SM, Rebeck GW. A beta species, including IsoAsp23 A beta, in Iowa-type familial cerebral amyloid angiopathy. *Acta Neuropathologica.* 2003; 105:252–258. [PubMed: 12557012]
12. Kameoka D, Ueda T, Imoto T. A method for the detection of asparagine deamidation and aspartate isomerization of proteins by MALDI/TOF-mass spectrometry using endoproteinase Asp-N. *J. Biochem.* 2003; 134:129–135. [PubMed: 12944379]
13. Rehder DS, Chelius D, McAuley A, Dillon TM, Xiao G, Crouse-Zeineddini J, Vardanyan L, Perico N, Mukku V, Brems DN, Matsumura M, Bondarenko PV. Isomerization of a single aspartyl residue of anti-epidermal growth factor receptor immunoglobulin gamma2 antibody highlights the role avidity plays in antibody activity. *Biochemistry.* 2008; 47:2518–2530. [PubMed: 18232715]
14. Ni W, Dai S, Karger BL, Zhou ZS. Analysis of isoaspartic Acid by selective proteolysis with Asp-N and electron transfer dissociation mass spectrometry. *Anal. Chem.* 2010; 82:7485–7491. [PubMed: 20712325]
15. Terashima I, Koga A, Nagai H. Identification of deamidation and isomerization sites on pharmaceutical recombinant antibody using (H<sub>2</sub>O)-O-18. *Anal. Biochem.* 2007; 368:49–60. [PubMed: 17617368]
16. Xiao G, Bondarenko PV, Jacob J, Chu GC, Chelius D. O-18 labeling method for identification and quantification of succinimide in proteins. *Anal. Chem.* 2007; 79:2714–2721. [PubMed: 17313184]
17. Li X, Cournoyer JJ, Lin C, O'Connor PB. Use of <sup>18</sup>O Labels to Monitor Deamidation during Protein and Peptide Sample Processing. *J. Am. Soc. Mass. Spectrom.* 2008; 19:855–864. [PubMed: 18394920]
18. Zhang W, Czupryn MJ. Analysis of isoaspartate in a recombinant monoclonal antibody and its charge isoforms. *J. Pharm. Biomed. Anal.* 2003; 30:1479–1490. [PubMed: 12467919]
19. Krokhn OV, Antonovici M, Ens W, Wilkins JA, Standing KG. Deamidation of -Asn-Gly-sequences during sample preparation for proteomics: Consequences for MALDI and HPLC-MALDI analysis. *Anal. Chem.* 2006; 78:6645–6650. [PubMed: 16970346]
20. De Boni S, Oberthur C, Hamburger M, Scriba GKE. Analysis of aspartyl peptide degradation products by high-performance liquid chromatography and high-performance liquid chromatography-mass spectrometry. *J. Chromatogr. A.* 2004; 1022:95–102. [PubMed: 14753775]
21. Winter D, Pipkorn R, Lehmann WD. Separation of peptide isomers and conformers by ultra performance liquid chromatography. *J. Sep. Sci.* 2009; 32:1111–1119. [PubMed: 19360781]
22. Lehmann WD, Schlosser A, Erben G, Pipkorn R, Bossemeyer D, Kinzel V. Analysis of isoaspartate in peptides by electrospray tandem mass spectrometry. *Protein Sci.* 2000; 9:2260–2268. [PubMed: 11152137]
23. Gonzalez LJ, Shimizu T, Satomi Y, Betancourt L, Besada V, Padron G, Orlando R, Shirasawa T, Shimonishi Y, Takao T. Differentiating alpha- and beta-aspartic acids by electrospray ionization and low-energy tandem mass spectrometry. *Rapid Commun. Mass Spectrom.* 2000; 14:2092–2102. [PubMed: 11114015]
24. Castet S, Enjalbal C, Fulcrand P, Guichou JF, Martinez J, Aubagnac JL. Characterization of aspartic acid and beta-aspartic acid in peptides by fast-atom bombardment mass spectrometry and tandem mass spectrometry. *Rapid Commun. Mass Spectrom.* 1996; 10:1934–1938.
25. Yamazaki Y, Fujii N, Sadakane Y. Differentiation and semiquantitative analysis of an isoaspartic acid in human alpha-Crystallin by postsource decay in a curved field reflectron. *Anal. Chem.* 2010; 82:6384–6394. [PubMed: 20669993]

26. Cournoyer JJ, Pittman JL, Ivleva VB, Fallows E, Waskell L, Costello CE, O'Connor PB. Deamidation: Differentiation of aspartyl from isoaspartyl products in peptides by electron capture dissociation. *Protein Sci.* 2005; 14:452–463. [PubMed: 15659375]
27. Sargaeva NP, Lin C, O'Connor PB. Identification of Aspartic and Isoaspartic Acid Residues in Amyloid beta Peptides, Including A beta 1–42, Using Electron-Ion Reactions. *Anal. Chem.* 2009; 81:9778–9786. [PubMed: 19873993]
28. Chan WYK, Chan TWD, O'Connor PB. Electron transfer dissociation with supplemental activation to differentiate aspartic and isoaspartic residues in doubly charged peptide cations. *J. Am. Soc. Mass. Spectrom.* 2010; 21:1012–1015. [PubMed: 20304674]
29. Cournoyer JJ, Lin C, Bowman MJ, O'Connor PB. Quantitating the relative abundance of isoaspartyl residues in deamidated proteins by electron capture dissociation. *J. Am. Soc. Mass. Spectrom.* 2007; 18:48–56. [PubMed: 16997569]
30. O'Connor PB, Cournoyer JJ, Pitteri SJ, Chrisman PA, McLuckey SA. Differentiation of aspartic and isoaspartic acids using electron transfer dissociation. *J. Am. Soc. Mass. Spectrom.* 2006; 17:15–19. [PubMed: 16338146]
31. Liu M, Cheetham J, Cauchon N, Ostovic J, Ni W, Ren D, Zhou ZS. Protein Isoaspartate Methyltransferase-Mediated 18O-Labeling of Isoaspartic Acid for Mass Spectrometry Analysis. *Anal. Chem.* 2011; 84:1056–1062. [PubMed: 22132761]
32. Yang HQ, Fung EYM, Zubarev AR, Zubarev RA. Toward proteome-scale identification and quantification of isoaspartyl residues in biological samples. *J. Proteome Res.* 2009; 8:4615–4621. [PubMed: 19663459]
33. Mukherjee R, Adhikary L, Khedkar A, Iyer H. Probing deamidation in therapeutic immunoglobulin gamma (IgG1) by 'bottom-up' mass spectrometry with electron transfer dissociation. *Rapid Commun. Mass Spectrom.* 2010; 24:879–884. [PubMed: 20196189]
34. Seebach D, Overhand M, Kuhnle FNM, Martinoni B, Oberer L, Hommel U, Widmer H. Beta-peptides: Synthesis by Arndt-Eistert homologation with concomitant peptide coupling. Structure determination by NMR and CD spectroscopy and by X-ray crystallography. Helical secondary structure of a beta-hexapeptide in solution and its stability towards pepsin. *Helv. Chim. Acta.* 1996; 79:913–941.
35. Appella DH, Christianson LA, Karle IL, Powell DR, Gellman SH. beta-peptide foldamers: Robust Helix formation in a new family of beta-amino acid oligomers. *J. Am. Chem. Soc.* 1996; 118:13071–13072.
36. Disney MD, Hook DF, Namoto K, Seeberger PH, Seebach D. N-linked glycosylated beta-peptides are resistant to degradation by glycoamidase A. *Chem. Biodiversity.* 2005; 2:1624–1634.
37. Seebach D, Beck AK, Bierbaum DJ. The world of beta- and gamma-peptides comprised of homologated proteinogenic amino acids and other components. *Chem. Biodiversity.* 2004; 1:1111–1239.
38. Weiss HM, Wirz B, Schweitzer A, Amstutz R, Perez MIR, Andres H, Metz Y, Gardiner J, Seebach D. ADME investigations of unnatural peptides: Distribution of a C-14-labeled beta(3)-octaarginine in rats. *Chem. Biodiversity.* 2007; 4:1413–1437.
39. Seebach D, Gardiner J. Beta-peptidic peptidomimetics. *Acc. Chem. Res.* 2008; 41:1366–1375. [PubMed: 18578513]
40. Kritzer JA, Lear JD, Hodsdon ME, Schepartz A. Helical beta-peptide inhibitors of the p53-hDM2 interaction. *J. Am. Chem. Soc.* 2004; 126:9468–9469. [PubMed: 15291512]
41. Namoto K, Gardiner J, Kimmerlin T, Seebach D. Investigation of the interactions of beta-peptides with DNA duplexes by circular dichroism spectroscopy. *Helv. Chim. Acta.* 2006; 89:3087–3103.
42. Seebach D, Matthews JL. Beta-peptides: a surprise at every turn. *Chem. Commun.* 1997:2015–2022.
43. Ben Hamidane H, Vorobyev A, Larregola M, Lukaszuk A, Tourwe D, Lavielle S, Karoyan P, Tsybin YO. Radical stability directs electron capture and transfer dissociation of beta-amino acids in peptides. *Chem. Eur. J.* 2010; 16:4612–4622. [PubMed: 20235239]
44. Sargaeva NP, Lin C, O'Connor PB. Unusual fragmentation of beta-linked peptides by ExD tandem mass spectrometry. *J. Am. Soc. Mass. Spectrom.* 2011; 22:480–491. [PubMed: 21472566]

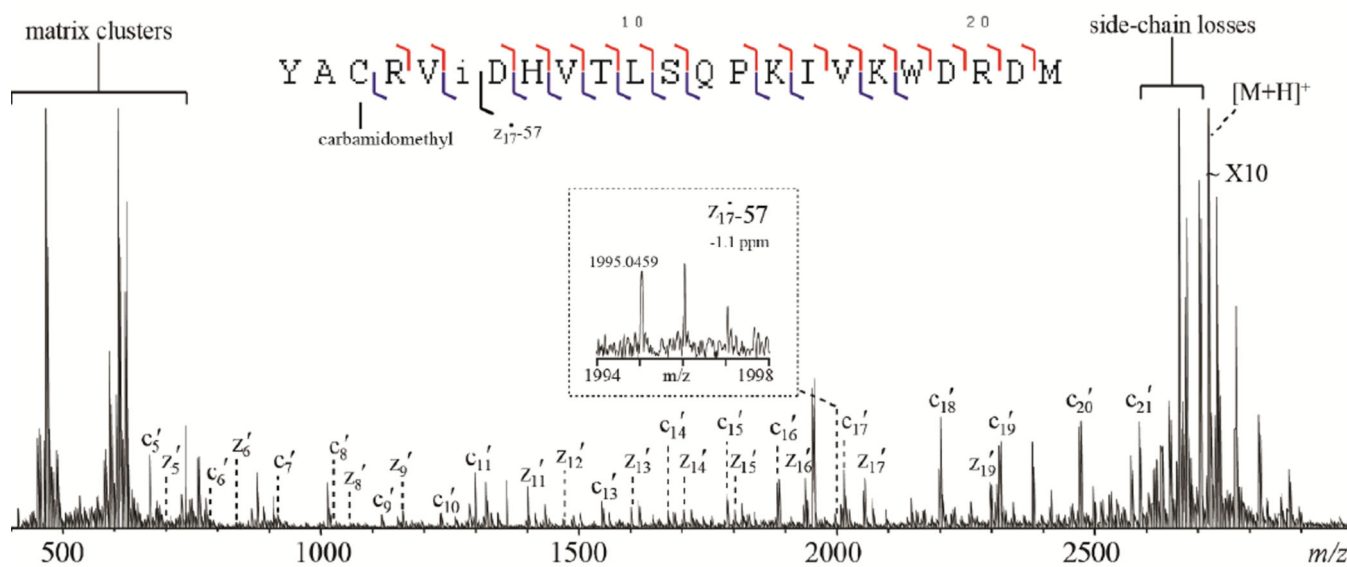
45. Brown RS, Lennon JJ. Sequence-Specific Fragmentation of Matrix-Assisted Laser-Desorbed Protein Peptide Ions. *Anal. Chem.* 1995; 67:3990–3999. [PubMed: 8633762]
46. Lennon JJ, Walsh KA. Direct sequence analysis of proteins by in-source fragmentation during delayed ion extraction. *Protein Sci.* 1997; 6:2446–2453. [PubMed: 9385647]
47. Asakawa D. Principles of hydrogen radical mediated peptide/protein fragmentation during matrix-assisted laser desorption/ionization mass spectrometry. *Mass Spectrom. Rev.* 2014
48. Takayama M. N-C-alpha bond cleavage of the peptide backbone via hydrogen abstraction. *J. Am. Soc. Mass. Spectrom.* 2001; 12:1044–1049.
49. Köcher T, Engström Å, Zubarev RA. Fragmentation of peptides in MALDI in-source decay mediated by hydrogen radicals. *Anal. Chem.* 2005; 77:172–177. [PubMed: 15623293]
50. Jagannadham MV, Nagaraj R. Detecting the site of phosphorylation in phosphopeptides without loss of phosphate group using MALDI TOF mass spectrometry. *Anal. Chem. Insights.* 2008; 3:21–29. [PubMed: 19609387]
51. Soltwisch J, Dreisewerd K. Discrimination of isobaric leucine and isoleucine residues and analysis of post-translational modifications in peptides by MALDI in-source decay mass spectrometry combined with collisional cooling. *Anal. Chem.* 2010; 82:5628–5635. [PubMed: 20524643]
52. Demeure K, Gabelica V, De Pauw EA. New Advances in the Understanding of the In-Source Decay Fragmentation of Peptides in MALDI-TOF-MS. *J. Am. Soc. Mass. Spectrom.* 2010; 21:1906–1917. [PubMed: 20832332]
53. Asakawa D, Smargiasso N, Pauw E. Discrimination of Isobaric Leu/Ile Residues by MALDI In-Source Decay Mass Spectrometry. *J. Am. Soc. Mass. Spectrom.* 2013; 24:297–300. [PubMed: 23307320]
54. Asakawa D, Calligaris D, Zimmerman TA, Pauw ED. In-Source Decay during Matrix-Assisted Laser Desorption/Ionization Combined with the Collisional Process in an FTICR Mass Spectrometer. *Anal. Chem.* 2013; 85:7809–7817. [PubMed: 23879863]
55. Nicolardi S, Switzar L, Deelder AM, Palmblad M, van der Burgt YE. Top-down MALDI-in-source decay-FTICR mass spectrometry of isotopically resolved proteins. *Anal. Chem.* 2015
56. Zubarev RA, Haselmann KF, Budnik B, Kjeldsen F, Jensen F. Towards an understanding of the mechanism of electron-capture dissociation: a historical perspective and modern ideas. *Eur. J. Mass Spectrom.* 2002; 8:337–350.
57. Demeure K, Quinton L, Gabelica V, De Pauw E. Rational selection of the optimum MALDI matrix for top-down proteomics by in-source decay. *Anal. Chem.* 2007; 79:8678–8685. [PubMed: 17939742]
58. Asakawa D, Takayama M. C(alpha) - C Bond Cleavage of the Peptide Backbone in MALDI In-Source Decay Using Salicylic Acid Derivative Matrices. *J. Am. Soc. Mass. Spectrom.* 2011; 22:1224–1233. [PubMed: 21953105]
59. Asakawa D, Takayama M. Specific cleavage at peptide backbone C(alpha)-C and CO-N bonds during matrix-assisted laser desorption/ionization in-source decay mass spectrometry with 5-nitrosalicylic acid as the matrix. *Rapid Commun. Mass Spectrom.* 2011; 25:2379–2383. [PubMed: 21793066]
60. Asakawa D, Takayama M. Fragmentation processes of hydrogen-deficient peptide radicals in matrix-assisted laser desorption/ionization in-source decay mass spectrometry. *J. Phys. Chem. B.* 2012; 116:4016–4023. [PubMed: 22372616]
61. Asakawa D, Sakakura M, Takayama M. Influence of initial velocity of analytes on in-source decay products in MALDI mass spectrometry using salicylic acid derivative matrices. *Int. J. Mass spectrom.* 2013; 337:29–33.
62. Li X, Yu X, Costello CE, Lin C, O'Connor PB. Top-Down Study of beta(2)-Microglobulin Deamidation. *Anal. Chem.* 2012; 84:6150–6157. [PubMed: 22746280]
63. Kjeldsen F, Haselmann KF, Budnik BA, Jensen F, Zubarev RA. Dissociative capture of hot (3–13 eV) electrons by polypeptide polycations: an efficient process accompanied by secondary fragmentation. *Chem. Phys. Lett.* 2002; 356:201–206.
64. Smargiasso N, Quinton L, De Pauw E. 2-Aminobenzamide and 2-aminobenzoic acid as new MALDI matrices inducing radical mediated in-source decay of peptides and proteins. *J. Am. Soc. Mass. Spectrom.* 2012; 23:469–474. [PubMed: 22183958]

65. Asakawa D, Calligaris D, Smargiasso N, De Pauw E. Ultraviolet laser induced hydrogen transfer reaction: study of the first step of MALDI in-source decay mass spectrometry. *J. Phys. Chem. B.* 2013; 117:2321–2327. [PubMed: 23360482]
66. Anusiewicz I, Jasionowski M, Skurski P, Simons J. Backbone and side-chain cleavages in electron detachment dissociation (EDD). *J. Phys. Chem. A.* 2005; 109:11332–11337. [PubMed: 16331920]
67. Kjeldsen F, Silivra OA, Ivonin IA, Haselmann KF, Gorshkov M, Zubarev RA. C $\alpha$ -C Backbone Fragmentation Dominates in Electron Detachment Dissociation of Gas Phase Polypeptide Polyanions. *Chem. Eur. J.* 2005; 11:1803–1812. [PubMed: 15672435]
68. Soltwisch J, Souady J, Berkenkamp S, Dreisewerd K. Effect of gas pressure and gas type on the fragmentation of peptide and oligosaccharide ions generated in an elevated pressure UV/IR-MALDI ion source coupled to an orthogonal time-of-flight mass spectrometer. *Anal. Chem.* 2009; 81:2921–2934. [PubMed: 19301914]
69. O'Connor PB, Costello CE. A high pressure matrix-assisted laser desorption/ionization Fourier transform mass spectrometry ion source for thermal stabilization of labile biomolecules. *Rapid Commun. Mass Spectrom.* 2001; 15:1862–1868. [PubMed: 11565105]

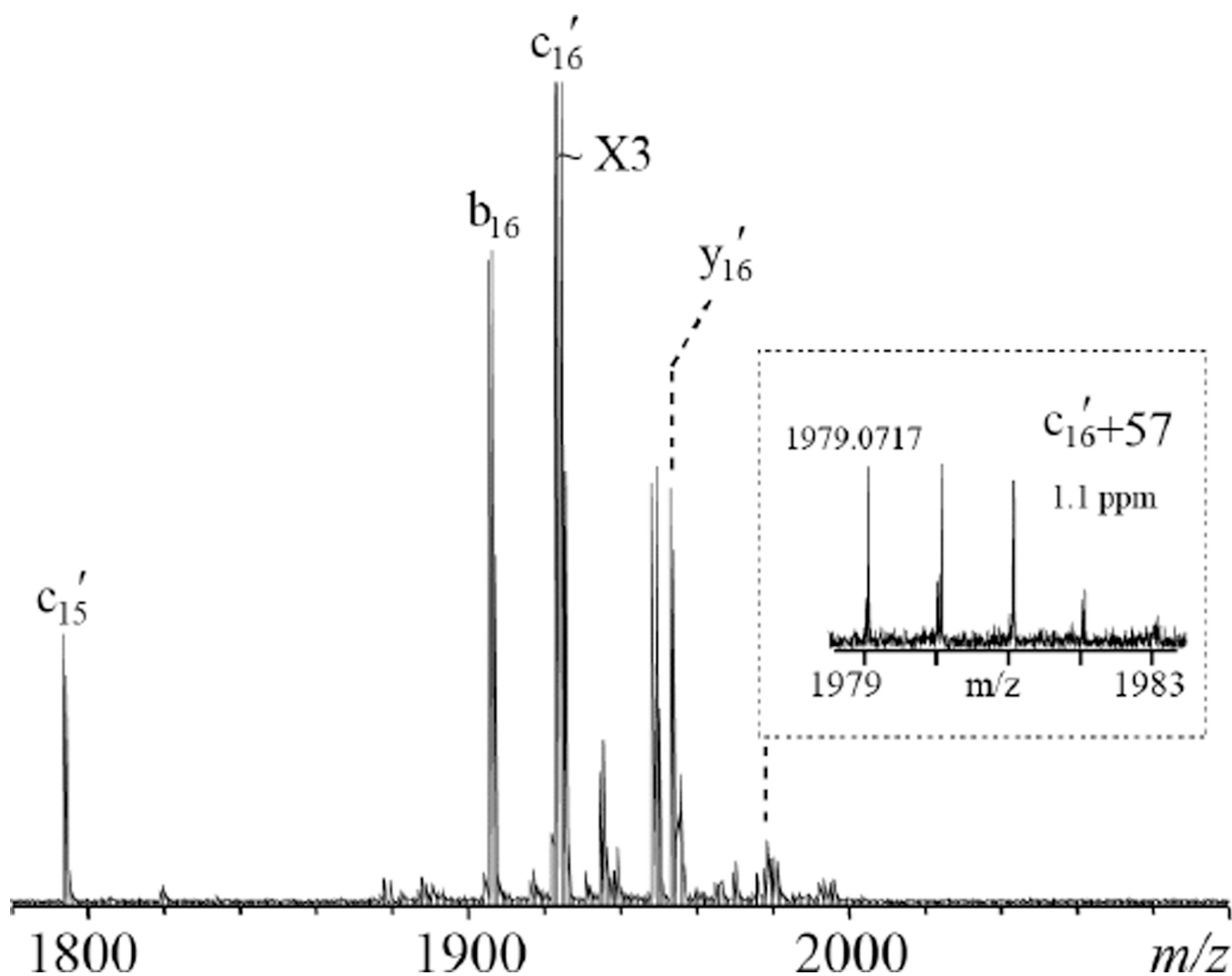




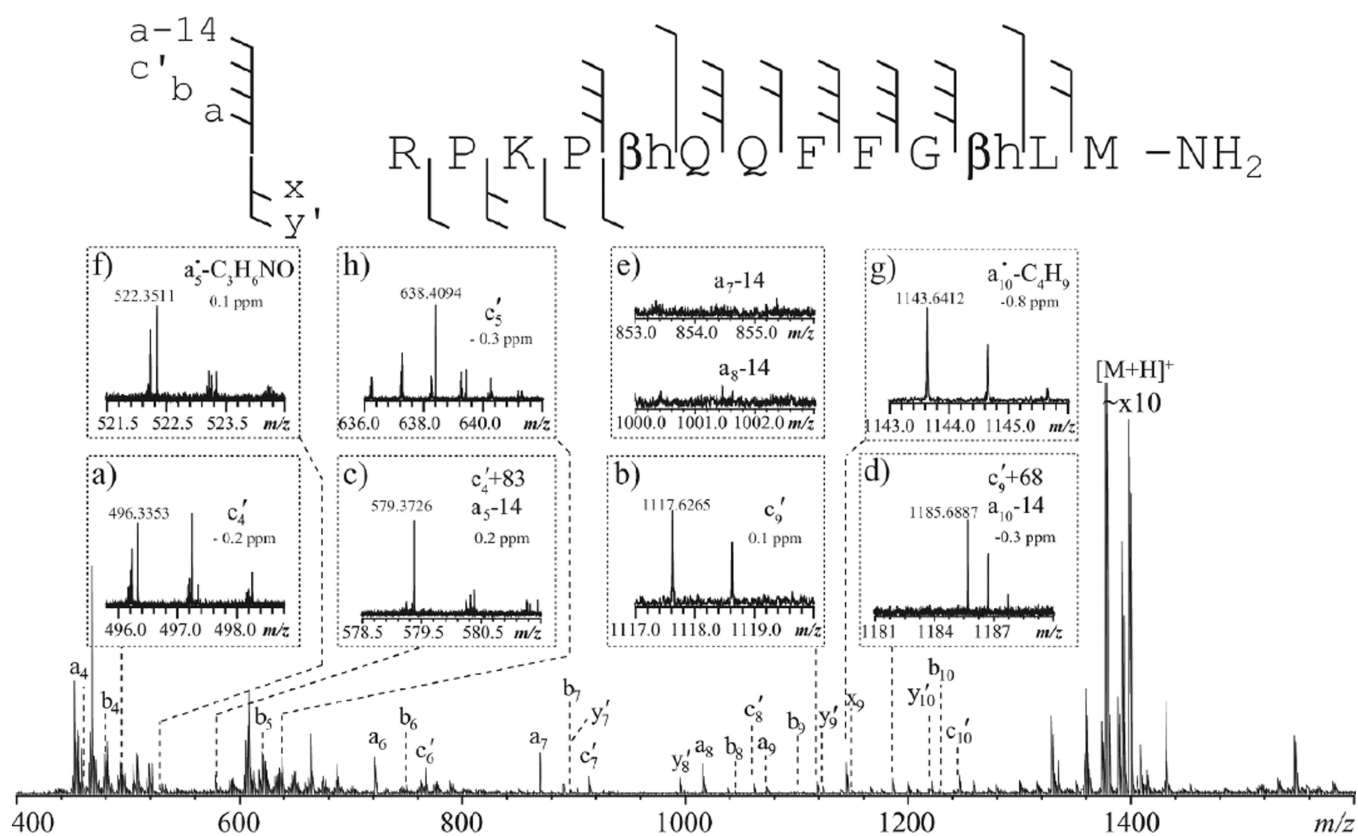
**Figure 1.** The ISD spectrum of the aged  $\beta$ 2M peptide (1–36) using the 1,5-DAN/2-PA matrix, obtained on the MALDI-FTICR mass spectrometer. Insets show the zoomed-in view of the spectral region corresponding to the isoAsp17-diagnostic ion in the ISD spectra of (a) the aged and (b) the unaged sample.



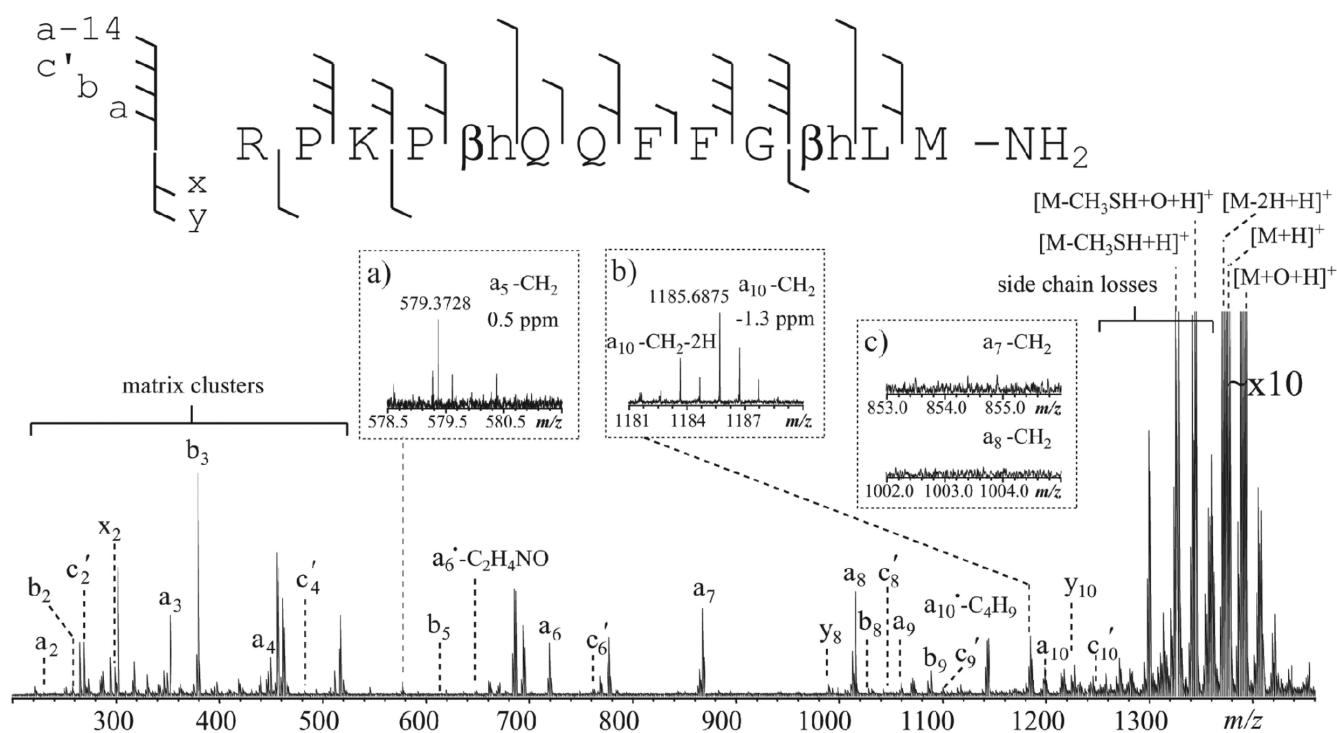
**Figure 2.** The ISD spectrum of the aged  $\beta$ 2M peptide (78–99) using the 1,5-DAN/2-PA matrix, obtained on the MALDI-FTICR mass spectrometer. Inset shows the zoomed-in view of the spectral region corresponding to the isoAsp83-diagnostic ion.



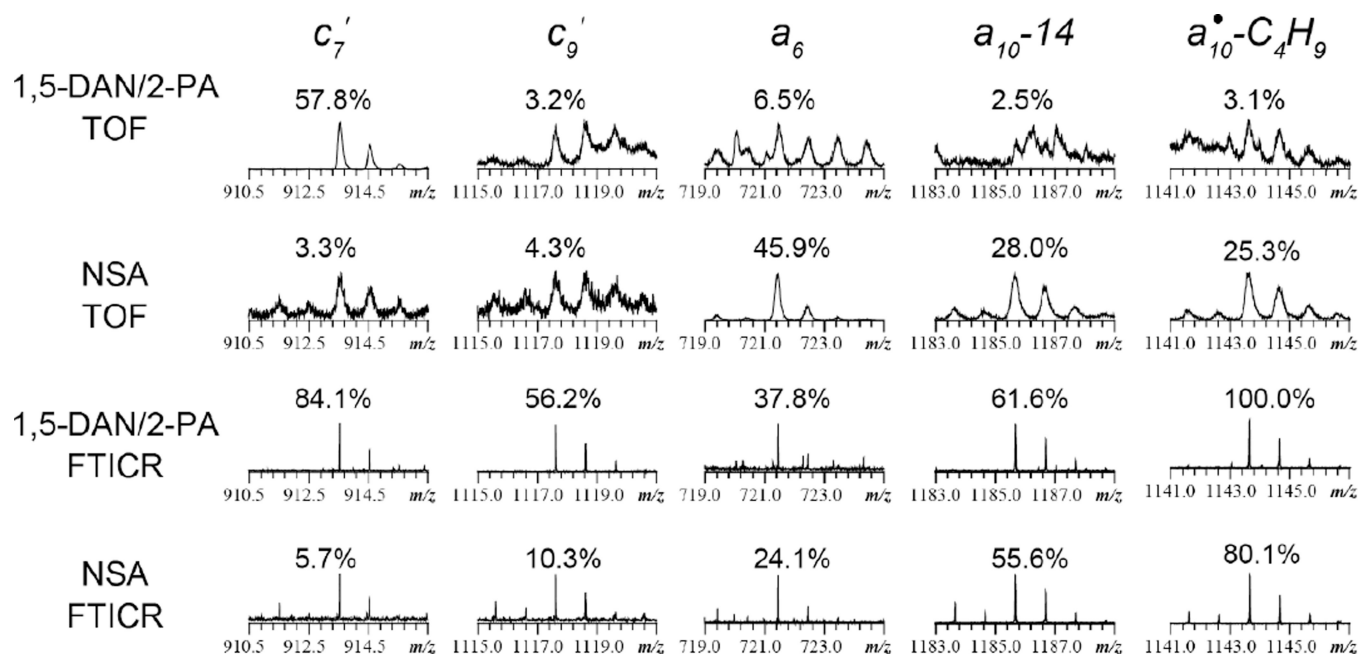
**Figure 3.** The ISD spectrum of the aged  $\beta$ 2M protein using the 1,5-DAN/2-PA matrix, with selective accumulation of ions within the  $m/z$  range of 1850 to 2050, obtained on the MALDI-FTICR mass spectrometer. Inset shows the zoomed-in view of the spectral region corresponding to the isoAsp17-diagnostic ion.



**Figure 4.** The ISD spectrum of the  $\beta$ -substance P analogue using the 1,5-DAN/2-PA matrix, obtained on the MALDI-FTICR mass spectrometer. Insets show the zoomed-in view of several spectral regions of interest.

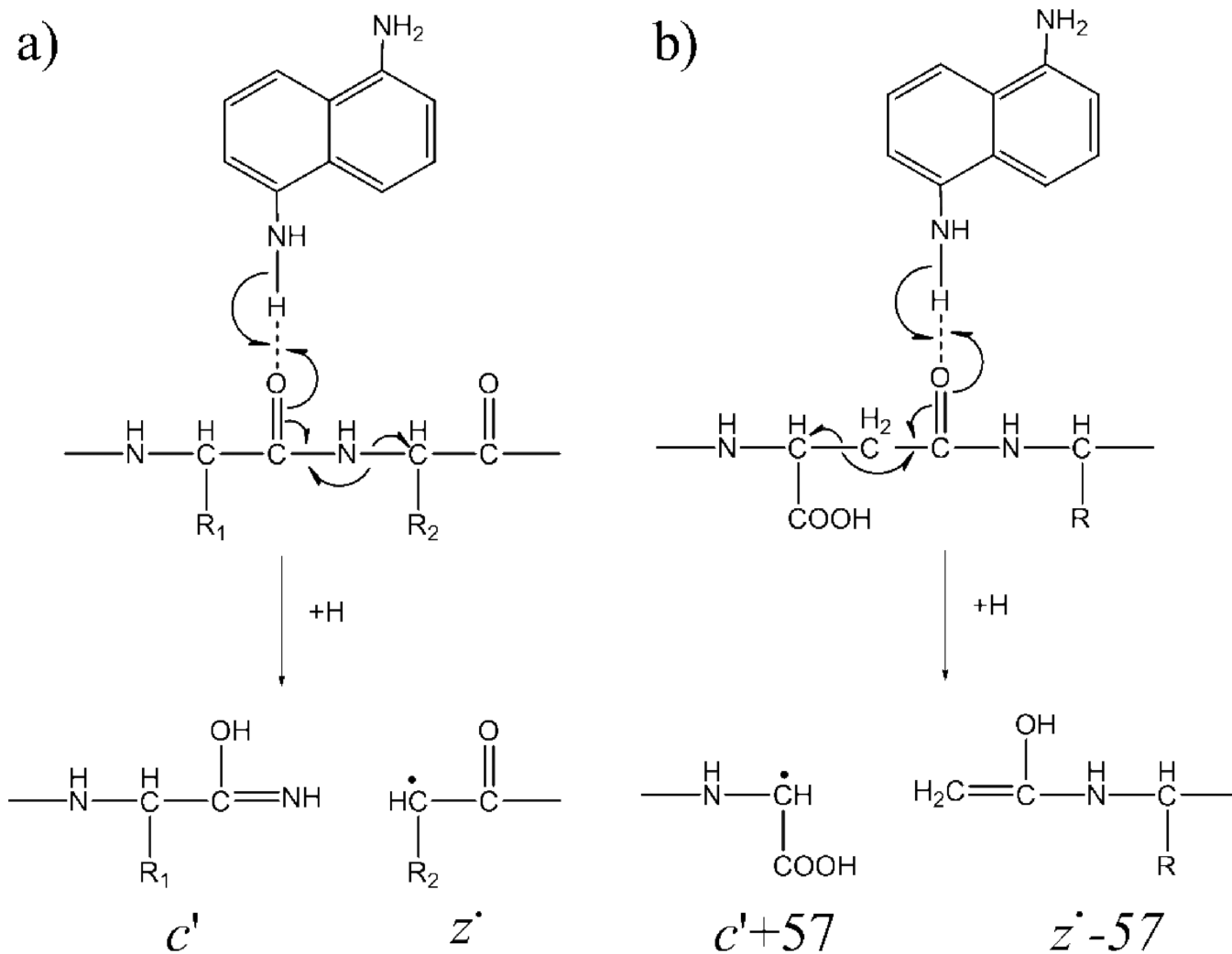


**Figure 5.**  
The ISD spectrum of the  $\beta$ -substance P analogue using the 5-NSA matrix, obtained on the MALDI-FTICR mass spectrometer. Insets show the zoomed-in view of several spectral regions of interest.

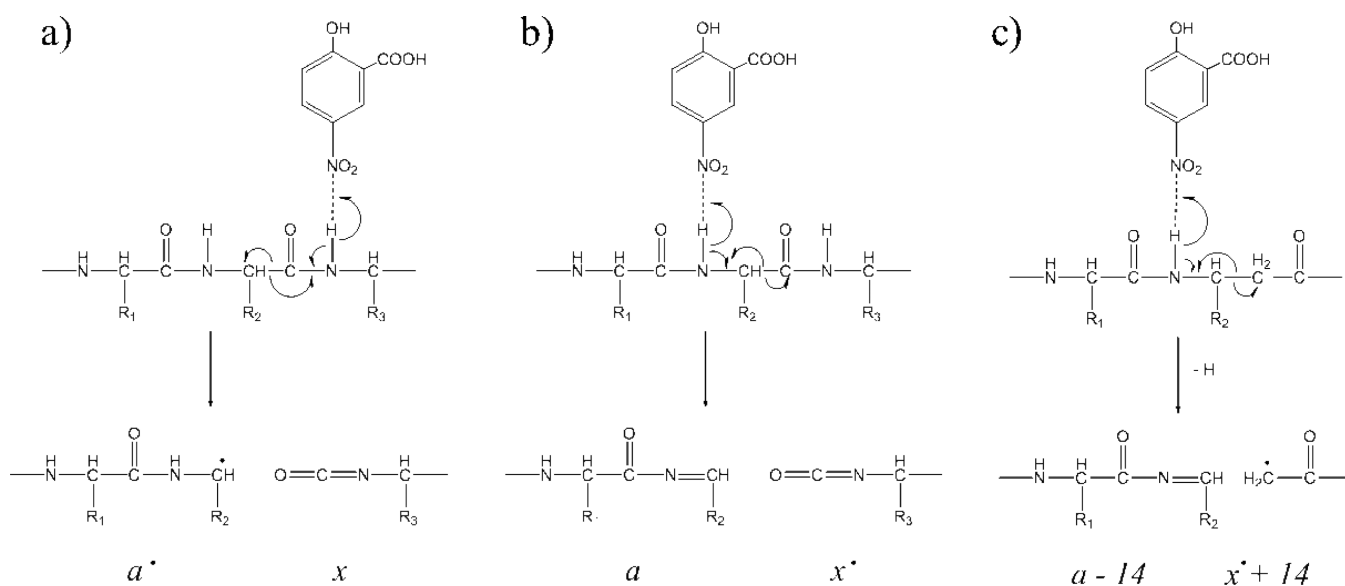


**Figure 6.** Zoomed-in views of several regions of interest in the ISD spectra of  $\beta$ -substance P analogue obtained with the 1,5-DAN/2-PA and 5-NSA matrices, and on the TOF and FTICR instruments, respectively.



**Scheme 1.**

Proposed mechanisms for ISD with the 1,5-DAN matrix: (a) formation of the  $c'/z'$  ions, and (b) formation of the isoAsp-diagnostic ions.

**Scheme 2.**

Proposed mechanisms for ISD with the 5-NSA matrix: (a) formation of the  $a^*/x$  ions, (b) formation of the  $a/x^*$  ions, and (c) formation of the  $a-14$  ion diagnostic of the  $\beta_3$ -linkage.